RESEARCH ARTICLE

Synthesis of $Zn_2(BDC)_2(DABCO)$ MOF by solution and solvothermal methods and evaluation of its anti-bacterial

Yasaman Rahvar[1], Negar Motakef-Kazemi[1,*], Reza Hosseini Doust[2]

[1] Department of Medical Nanotechnology, Faculty of Advanced Sciences and Technology, Tehran Medical Sciences, Islamic Azad University, Tehran, Iran.

[2] Department of Microbiology, Faculty of advanced sciences & biotechnology, Tehran Medical Sciences, Islamic Azad University, Tehran, Iran.

ARTICLE INFO

Article History:
Received 23 Jul 2021
Accepted 15 Oct 2021
Published 01 Nov 2021

Keywords:
MOF
Solution method
Solvothermal method
Anti-bacterial activity

ABSTRACT

Objective(s): In recent years, nanomaterials with anti-bacterial activity have acted as antibiotics, and a new method of nanotechnology treatment is available. Nanoparticles (NPs) are effective against drug-resistant strains. Metal-organic frameworks (MOFs) are highly porous composite materials with attractive applications. This material has attracted a lot of attention due to its unique properties such as anti-bacterial application. $Zn_2(BDC)_2(DABCO)$ MOF is a Zn-MOF based organic framework (Zn-MOF) with various applications.

Methods: In the present study, this Zn-MOF was synthesized by solution at room temperature and solvothermal at 90 ºC methods. The samples were characterized by Fourier transform infrared (FTIR), X-ray diffraction (XRD), dynamic light scattering (DLS), zeta potential, field emission scanning electron microscopy (FESEM), and diffuse reflection spectroscopy (DRS). Finally, the anti-bacterial activities of samples were investigated against Escherichia coli (*E. coli*) as gram-negative bacteria and Staphylococcus aureus (*S. aureus*) as gram-positive bacteria.

Results: FTIR and XRD results were evaluated functional groups and crystal structure respectively. DLS and zeta potential results were studied size and distribution diagram, and surface charge respectively. The morphology and size were observed by SEM images in the nanometer scale. The Ultraviolet (UV) protective property and band gap energy were investigated by DRS absorption. The antibacterial activity was confirmed against *E. coli* were and *S. aureus*.

Conclusions: This work showed that $Zn_2(BDC)_2(DABCO)$ MOF can be a good candidate for medicinal applications.

How to cite this article
Rahvar Y., Motakef-Kazemi N., Hosseini Doust R. Synthesis of $Zn_2(BDC)_2(DABCO)$ MOF by solution and solvothermal methods and evaluation of its anti-bacterial. Nanomed Res J, 2021; 6(4): 360-368. DOI: 10.22034/nmrj.2021.04.006

INTRODUCTION

Today, nanotechnology is expanding in different fields and increasing the potential benefits of application in the world [1]. The dimensional range of nanoparticles is between 1-100 nm, and the small size and large surface area opens up new approaches for various sciences [2]. In recent years, the study of nanoparticles with antimicrobial activity has increased due to the increased incidence of nosocomial infections and food poisoning caused by food pathogens [3]. Bacterial infections are one of the global public health concerns and place a heavy economic burden on a country's health care, and nanomaterials have emerged as potential antimicrobial agents [4]. The antimicrobial mechanism of nanoparticles is generally described by three models involving the induction of oxidative stress, the release of metal ion, and non-oxidative [5]. Human infections are the result of gram-negative and gram-positive bacteria, and bacterial-susceptible strains are used to accurately determine the anti-bacterial activity of NPs [6]. Among these, the nanoparticles of zinc

* Corresponding Author Email: *motakef@iaups.ac.ir*

oxide are one of the NPs that has high anti-bacterial potential and are important concerning gram-positive and gram-negative bacteria [7].

The metal organic frameworks as a class of porous hybrids, has the desired size and shape of pores. MOFs are synthesized through self-assembly metal centers (including metal ions or metal clusters) and linkers (including bridging ligands ([8]. Metal organic frameworks have promising usage in many fields, such as protein immobilization [9], catalysis [10, 11], photocatalytic [12], sorbent [13], gas storage and separation [14], luminescence [15], sensing [16], ion exchange [17], biomedicine [18], magnetism [19], drug delivery [20, 21], preparation of nanoparticles [22, 23], and anti-bacterial [24]. The release of metal ions from MOF structure makes them attractive antimicrobials for adjustable antibiotic applications [25]. The metal organic frameworks prepare by different methods such as solution [8], hydrothermal [27], solvothermal [26], diffusion [28], microwave [29], sonochemical [30], electrochemical [31], mechanochemical [32], ion thermal [33], microfluidic [34], and laser ablation [35, 36]. MOF components can be connected with several types of connections. These types of bonds involve metal coordination, hydrogen bonding, electrostatic interactions, and π-π stacking that can show adjustable structures, compounds, and properties [37]. The antimicrobial activity of MOFs is attributed to the presence of metal ions, such as Ag [38] and Zn [22]. Zinc as a non-toxic metal is widely used in many drugs and cosmetics. Also, it has properties such as a cicatrizing agent and skin moisturizer with anti-dandruff, astringent, anti-inflammatory and anti-bacterial [39]. Among the various MOFs, $Zn_2(BDC)_2(DABCO)$ (BDC = 1,4- benzenedicarboxylic acid, DABCO = 1,4-diazabicyclo [2.2.2] octane) is common Zn-MOF with large surface area [8, 26]. In $[Zn_2(BDC)_2(DABCO)].4DMF.1/2H_2O$ MOF, di-nuclear Zn_2 units are bridged by BDC to form a distorted 2D square grid $[Zn_2(BDC)]$, which is pillared by DABCO ligand to form a $\alpha\alpha$-Po type 3D network [40]. In this study, $Zn_2(BDC)_2(DABCO)$ was prepared by the methods of solution and thermal solution. Developing of the anti-bacterial properties of $Zn_2(BDC)_2(DABCO)$ MOF is the main purpose of this project.

MATERIALS AND METHODS

Materials

All materials were purchased without purification from Merck (Darmshtadt, Germany). Zinc acetate dihydrate ($Zn(OAc)_2{\cdot}2H_2O$) as metal ion, 1,4 benzenedicarboxylic acid (bdc) and 1,4-diazabicyclo[2.2.2] octane (dabco) as organic linkers, dimethylformamide (DMF) as solvents.

Synthesis of $Zn_2(BDC)_2(DABCO)$ MOF

In a normal reaction, 0.132 g Zn $(OAc)_2.2H_2O$ (2 mmol), 0.1 g BDC (2 mmol) and 0.035 g DABCO (1 mmol) were mixed to 25 ml DMF [8]. The optimal ratios of metal, chelating ligand and bridging ligand were 2:2:1. The sample was mixed for 30 minutes at 25 °C and at 90 °C. After filtration of the reaction mixture and washing the white crystals by solvent to remove any metal and ligand remaining, DMF was removed from white crystals by a furnace at 120 °C for 5 h [11].

Characterization

The prepared samples were analyzed by XRD, FTIR, UV blocking, DLS, and SEM. FTIR was obtained by utilizing a Spectrum Two (PerkinElmer-USA) using KBr disks for investigation functional groups. The diffraction of X-ray was performed for the estimation of samples in terms of crystalline structure by utilizing Cu Kα X-ray radiation with a voltage of 40 kV and a current of 30 mA by X'pert pro diffractometer (Panalytical). DLS was used for the samples size and size distribution (Zetasizer, England). The investigation of zeta potential of samples was performed by Zetasizer model Malvern company (England). Field emission scanning electron microscopy was utilized to observe the shape and size of the MOFs (Sigma VP, ZEISS). For the investigation of UV protective and energy gap (UV2550, Shimadzu), the spectroscopy of diffuse reflection was used. The anti-bacterial properties of samples were estimated by the method of disk diffusion against Escherichia coli (ATCC 1399, Islamic Azad University) and Staphylococcus aureus (ATCC 25923, Islamic Azad University).

RESULTS AND DISCUSSION

FTIR

The IR spectra of samples in the range of 400–4000 cm^{-1} were noted. FTIR spectra of $Zn_2(BDC)_2(DABCO)$ shows at 25 °C (Fig. 1a) and 90 °C (Fig. 1b). The stretch vibrations of O-H was observed at 3445 cm^{-1}. The high intensity peak of C=O at 1385 cm^{-1} are assigned to carboxylic groups. The aromatic bands of C–H are displayed at 3400 cm^{-1} however the band of hydroxyl functional group

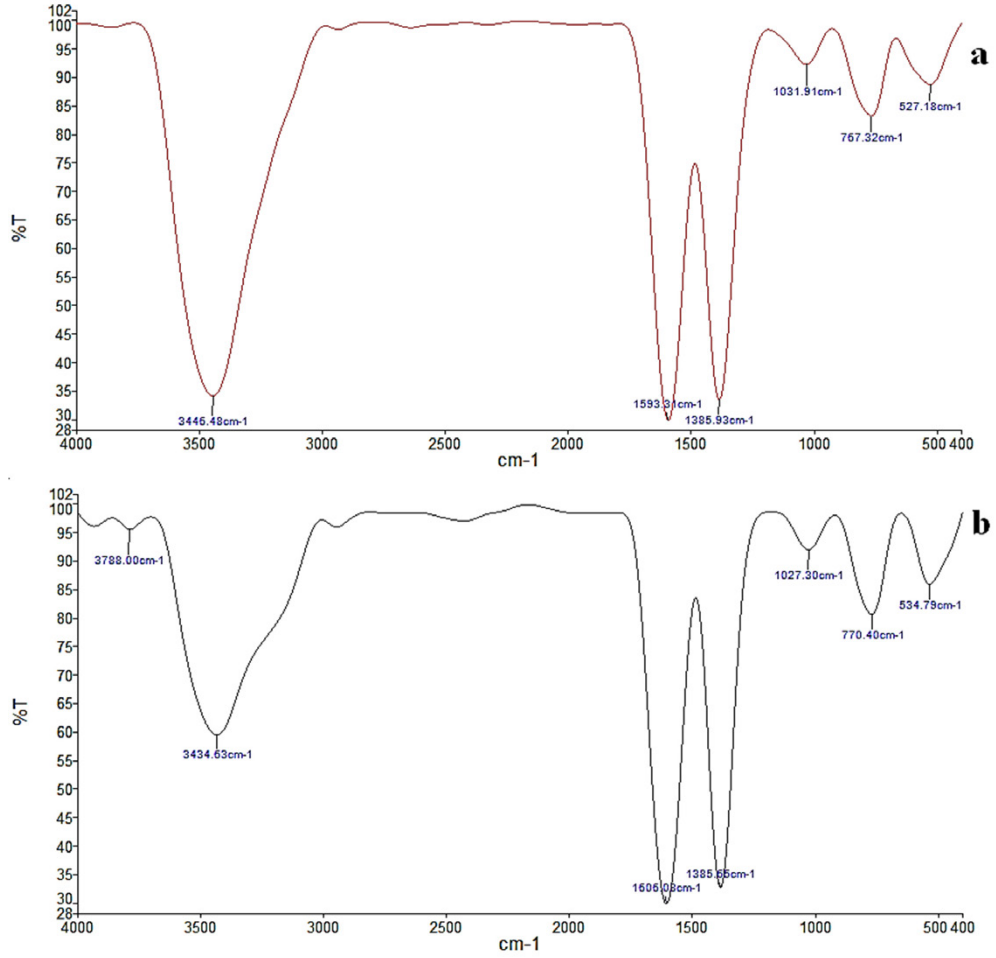

Fig. 1. FTIR spectra of MOF by a) solution and b) solvothermal method.

is presented at 2960 cm^{-1}. The CO_2 peak was appear at 2357 cm^{-1} which exist in environment. C=O stretch band is assigned at 1600 cm^{-1}. The carboxylic groups are assigned at 1387 cm^{-1} with the high intensity peak. As a result, $Zn_2(BDC)_2(DABCO)$ MOF results confirm previous reports [8, 26]. Hence, the FTIR results confirm the quality of the MOF synthesis.

XRD

X-ray diffraction of $Zn_2(BDC)_2(DABCO)$ was investigated from 5 to 80 (2θθ°), which demonstrated the structure of cubic crystal (Fig. 2). According to the XRD analysis, MOFs are synthesized acceptably and the structure of obtained crystal is near to the previous report [8, 26]. The XRD results confirm the structure of crystal for synthetic MOF.

DLS

The particle size of samples and distribution diagram were estimated by DLS. The results indicated a single-peak at 643 nm with slight distribution at 25 °C (Fig. 3a), and single peak at 683 nm with narrow distribution at 90 °C (Fig. 3b). These results were first reported for $Zn_2(BDC)_2(DABCO)$ MOF. The DLS results confirm the narrow size distribution of the synthetic MOF.

According to the results, higher synthesis temperature is caused to the growth increase of the MOF. The zeta potential was -14.1 (Fig. 4a) and -7.96 mV (Fig. 4b) at 25 ℃ and 90 ℃ respectively. Based on the results, the MOF is more stable at room temperature and the particle size is smaller. Zeta potential results were first reported for $Zn_2(BDC)_2(DABCO)$ MOF.

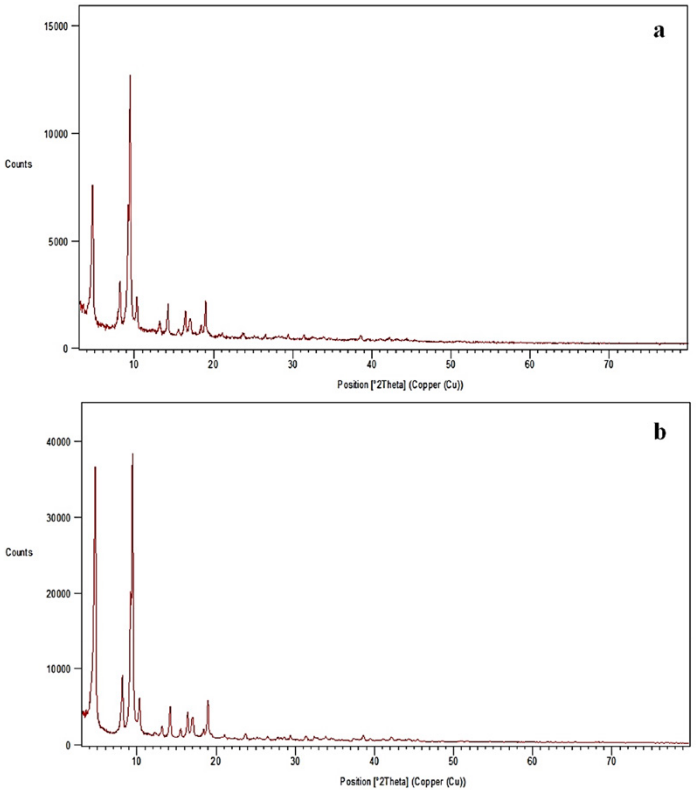

Fig. 2. XRD pattern of MOF by a) solution and b) solvothermal method.

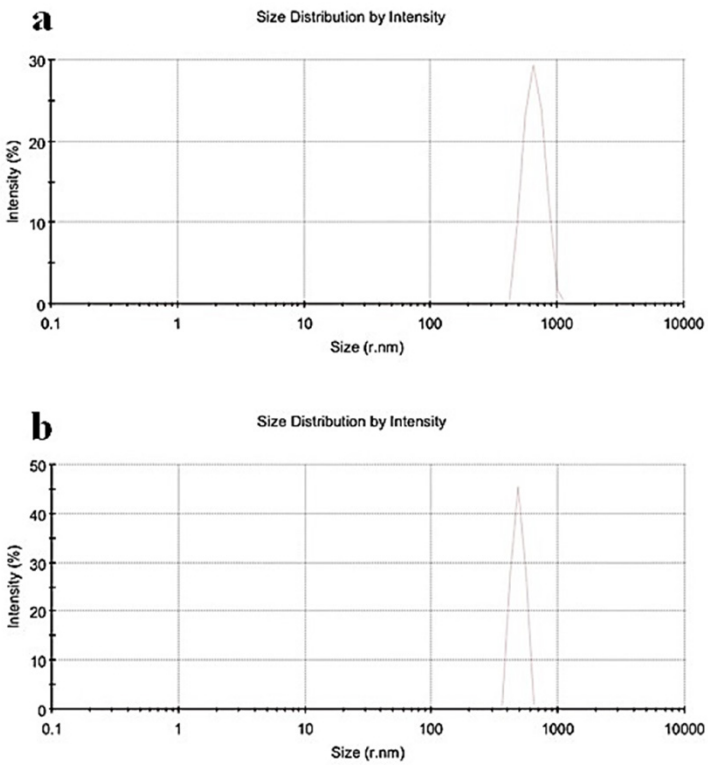

Fig. 3. DLS of MOF by a) solution and b) solvothermal method.

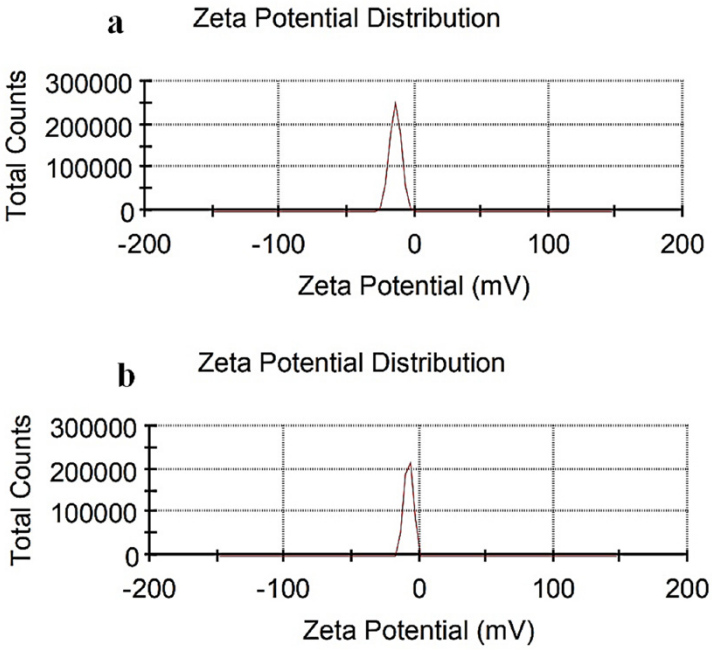

Fig. 4. Zeta potential of MOF by a) solution and b) solvothermal method.

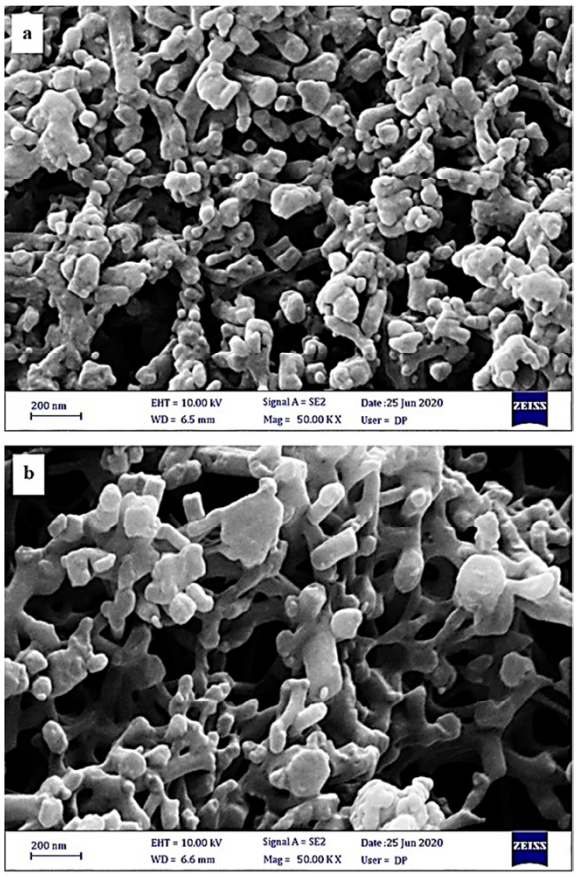

Fig. 5. FESEM images of MOF by a) solution and b) solvothermal method.

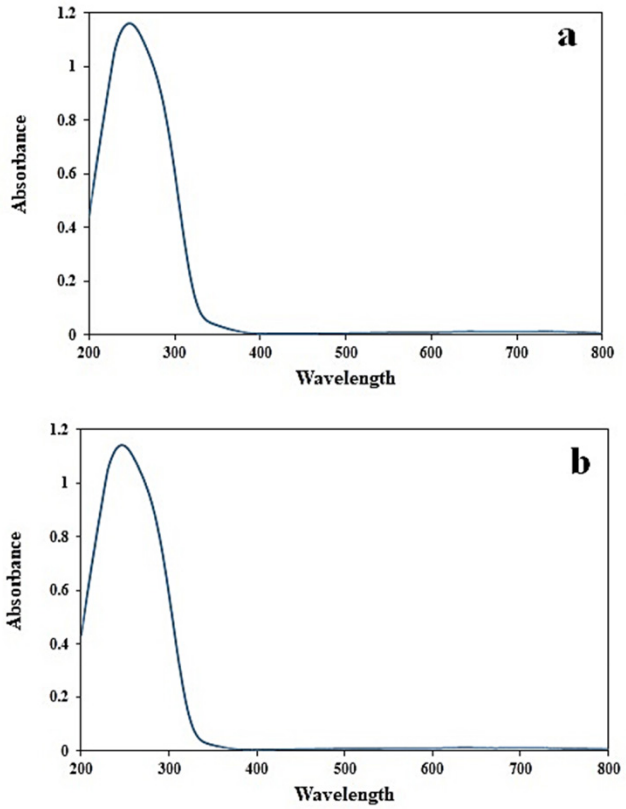

Fig. 6. DRS spectrum of MOF by a) solution and b) solvothermal method.

FESEM

The FESEM images of $Zn_2(BDC)_2(DABCO)$ at 25 ℃ and 90 ℃ are shown in Fig. 5. The images revealed that the structures are cubic shaped with smooth surface with nanometer in diameter [8, 26]. The obtained results showed that the size of MOF particle is smaller at room temperature and confirms the DLS results. Consequently, higher temperatures can cause particle growth and size to increase.

DRS

The spectra absorption of DRS was used to evaluation of the optical properties of $Zn_2(BDC)_2(DABCO)$ (Fig. 6). The MOF absorption of spectra was noted in the wavelength range of 200–800 nm in diffuse reflectance mode. The peak of absorption in the range of 200-400 nm was observed, which exhibited the protective properties of $Zn_2(BDC)_2(DABCO)$ samples. DRS results were first reported for $Zn_2(BDC)_2(DABCO)$ MOF.

The energy difference (in electron volts) between the highest capacitance band and the lowest conductance band is called the forbidden band energy or energy gap. Due to the band gap energies by the Tauc method as the transfer spectra of samples, MOF nanostructures were extracted. The band gap energies of MOF are approximately 3.6 and 3.55 eV at 25 ℃ and 90 ℃ respectively (Fig. 7). The obtained results showed that reducing the size increases the energy gap and is consistent with the previous report [41].

Anti-bacterial activity

The method of agar diffusion with the certain concentration (0.01 g/ml) was used to the investigation of $Zn_2(BDC)_2(DABCO)$ anti-bacterial activity against *E. coli* and *S. aureus*. The zone of inhibition was measured 9 mm at room temperature and 8 mm at 90°C for *Escherichia Coli* and 8 mm at room temperature and 7 mm at 90°C for *Staphylococcus aureus*. Many parameters such as concentration, morphology, particle size, and surface modifications affect the anti-bacterial activity. The results are based on previous reports [22, 42]. The principal mechanisms of MOF for anti-bacterial activity involve: the contact of bacterial

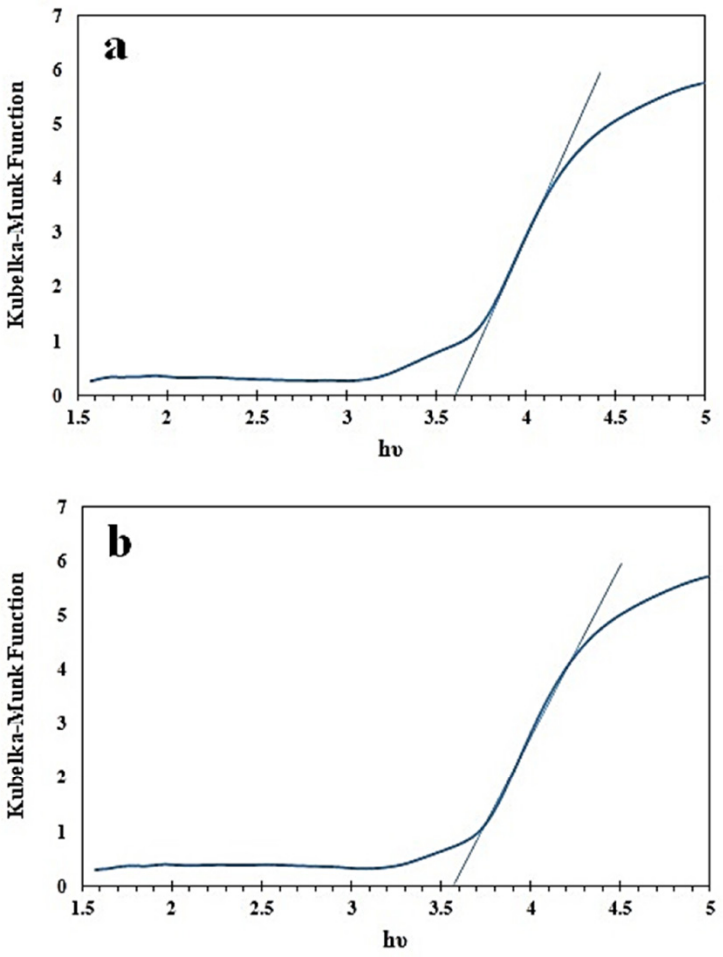

Fig. 7. The Munk-Kubelka function in terms of hν of MOF by a) solution and b) solvothermal method.

through cell walls and cell destruction of it, the production of reactive oxygen species (ROS), and the release of Zn^{+2} ions as an antimicrobial ion [43]. Anti-bacterial activity can affected be the release of COO^- and Zn^{+2} ions, metallic Zn, and amine group. According to the results, it has more anti-bacterial activity against the MOF at ambient temperature due to its smaller size and gram-negative bacteria because of more absorption of opposite charge. Anti-bacterial activity results were first reported for $Zn_2(BDC)_2(DABCO)$ MOF.

CONCLUSION

The $Zn_2(BDC)_2(DABCO)$ MOF homogeneous samples. The purity of crystalline structure of MOF was confirmed by XRD spectrum. The applications of anti-bacterial activity and UV blocking of MOF, successfully were observed in this research. Based on the results, the solution method produces particles with smaller size, more band gap energy and higher anti-bacterial activity. The solution method as a simple synthesis can be used in various fields of biological application such as cosmetic, pharmaceutical, food, etc., and become an important research field in the future. Despite the material cost for industrial applications, the synthesis results in a very short time are very encouraging synthesized by solution and thermal solution methods. The DLS and SEM results showed.

CONFLICTS OF INTEREST

The authors declare that there are no conflicts of interest.

REFERENCES

[1] McNeil SE. Nanotechnology for the biologist, J Leukoc Biol. 2005;78(3):585-594.

[2] Bhardwaj N, Pandey SK, Mehta J, Bhardwaj SK, Kim KH, Deep A. Bioactive nano-metal-organic frameworks as antimicrobials against gram-positive and gram-negative bacteria, Toxicol Res. 2018;7(5):931-941.
[3] Guerrero Correa M, Martínez FB, Patiño Vidal C, Streitt C, Escrig J, Lopez de Dicastillo C. Antimicrobial metal-based nanoparticles: a review on their synthesis, types and antimicrobial action, Beilstein J Nanotechnol. 2020;11:1450–1469.
[4] Ebnerasool FS, Motakef Kazemi N. Preparation and characterization of chitosan nanocomposite based on nanoscale silver and nanomontmorillonite, AMECJ. 2019;2(2):5-12.
[5] Leung YH, Ng AM, Xu X, Shen Z, Gethings LA, Ting Wong M, Chan CMN, Yao Guo M, Hang Ng Y, Djurišić AB, Lee PKH, Kin Chan W, Hong Yu L, Lee Phillips D, Ma APY, Leung FCC. Mechanisms of antibacterial activity of MgO: non-ROS mediated toxicity of MgO nanoparticles towards Escherichia coli, Small. 2014;10(6):1171–1183.
[6] Wang L, Hu C, Shao L. The antimicrobial activity of nanoparticles: present situation and prospects for the future, Int J Nanomedicine. 2017;12:1227–124
[7] Gudkov SV, Burmistrov DE, Serov DA, Rebezov MB, Semenova AA, Lisitsyn AB. A mini review of antibacterial properties of ZnO nanoparticles, Front Phys. 2021;9:1-12.
[8] Motakef Kazemi N, Shojaosadati SA, Morsali A. In situ synthesis of a drug-loaded MOF at room temperature, Micropor Mesopore Mat. 2014;186:73-79.
[9] Mehmandoust MR, Motakef kazemi N, Ashouri F. Nitrate adsorption from aqueous solution by metal-organic framework MOF-5, Iran J Sci Technol Trans A Sci. 2019;43(2):443-449.
[10] Nabipour H, Sadr Hossaini M, Rezanejade Bardajee G. Release behavior, kinetic and antimicrobial study of nalidixic acid from $[Zn_2(bdc)_2(dabco)]$ metal-organic frameworks, J Coord Chem. 2017;70(16):2771-2784.
[11] Ghourchian F, Motakef-Kazemi N, Ghasemi E, Ziyadi H. Zn-based MOF-chitosan-Fe_3O_4 nanocomposite as an effective nano-catalyst for azo dye degradation, J Environ Chem Eng. 2021;9(6):106388.
[12] Abrodi M, Homayoun Keihan A. Comparative photocatalytic performance of TiO_2 and TiO_2/en-MIL-101 (Cr) for degradation of rhodamine B as a model of pollutant under UV and visible irradiations, J Nanostruct. 2020;10(4):802-809.
[13] Motakef-Kazemi N. A novel sorbent based on metal–organic framework for mercury separation from human serum samples by ultrasound assisted-ionic liquid-solid phase microextraction, AMECJ. 2019;2(3):67-78.
[14] Kitagawa S. Metal-organic frameworks (MOFs), Chem Soc Rev. 2014;43(16):5415-5418.
[15] Janiak C, Vieth JK. MOFs, MILs and more: concepts, properties and applications for porous coordination networks (PCNs), NJC. 2010;34(11):2366-2388.
[16] Lin ZJ, LÜ J, Hong M, Cao R. Metal-organic frameworks based on flexible ligands (FL-MOFs): structures and applications, Chem Soc Rev. 2014;43(16):5867-5895.
[17] Kumar P, Pournara A, Kim KH, Bansal V, Rapti S, Manos MJ. Metal-organic frameworks: challenges and opportunities for ion-exchange/sorption applications, Prog Mater Sci. 2017;86:25-74.
[18] Horcajada P, Gref R, Baati T, Allan PK, Maurin G, Couvreur P, Ferey G, Morris RE, Serre C. Metal-organic frameworks in biomedicine, Chem Rev. 2012;112(2):1232-1268.
[19] Li S, Luo P, Wu H, Wei C, Hu Y, Qiu G. Strategies for improving the performance and application of MOFs photocatalysts, Chem Cat Chem. 2019;11(13):2978-2993.
[20] Lazaro IA, Forgan RS. Application of zirconium MOFs in drug delivery and biomedicine, Coord Chem Rev. 2019;380:230-259.
[21] Wu YN, Zhou M, Li S, Li Z, Li J, Wu B. Li G, Li F, Guan X. Magnetic metal-organic frameworks: γγ-Fe_2O_3@MOFs via confined in situ pyrolysis method for drug delivery, Small. 2014;10(14):2927-2936.
[22] Hajiashrafi S, Motakef-Kazemi N. Preparation and evaluation of ZnO nanoparticles by thermal decomposition of MOF-5, Heliyon. 2019;5:e02152.
[23] Motakef-Kazemi N, Rashidian M, Taghizadeh Dabbagh S, Yaqoubi M. Synthesis and characterization of bismuth oxide nanoparticles by thermal decomposition of bismuth-based MOF and evaluation of its nanocomposite, Iran J Chem Chem Eng. 2021;40(1):11-19.
[24] Wyszogrodzka G, Marszałek B, Gil B, Dorożyński P. Metal-organic frameworks: mechanisms of antibacterial action and potential applications, Drug Discov Today. 2016;21(6):1009-1018.
[25] Quirós J, Boltes K, Aguado S, de Villoria RG, Vilatela JJ, Rosal R. Antimicrobial metal-organic frameworks incorporated into electrospun fibers, Chem Eng J. 2015;262:189-197.
[26] Motakef Kazemi N, Shojaosadati SA, Morsali A. Evaluation of the effect of nanoporous nanorods Zn2(bdc)2(dabco) dimension on ibuprofen loading and release, J Iran Chem. Soc. 2016;13(7):1205-1212.
[27] Yaghi OM, Li H. Hydrothermal synthesis of a metal-organic framework containing large rectangular channels, J Am Chem Soc. 1995;117(41):10401–10402.
[28] Al-Ghoul M, Issa R, Hmadeh M. Synthesis, size and structural evolution of metal–organic framework-199 via a reaction–diffusion process at room temperature, Cryst Eng Comm. 2017;19:608-612.
[29] Klinowski J, Almeida Paz FA, Silva P, Rocha J. Microwave-assisted synthesis of metal–organic frameworks, Dalton Trans. 2011;40:321-330.
[30] Son WJ, Kim J, Kim J, Ahn WS. Sonochemical synthesis of MOF-5, Chem Commun. 2008;47:6336-6338.
[31] Al-Kutubi H, Gascon J, Sudhölter EJR, Rassaei L. Electrosynthesis of metal–organic frameworks: challenges and opportunities, Chem Electro Chem. 2015;2(4):462-474.
[32] Wang Z, Li Z, Nga M, Milner PJ. Rapid mechanochemical synthesis of metal–organic frameworks using exogenous organic base, Dalton Trans. 2020;49:16238-16244.
[33] Liu C, Zhang G, Zhao C, Li X, Li M, Na H. MOFs synthesized by the ionothermal method addressing the leaching problem of IL–polymer composite membranes, Chem Commun. 2014;50:14121-14124.
[34] Echaide-Górriz C, Clément C, Cacho-Bailo F, Téllez C, Coronas J. New strategies based on microfluidics for the synthesis of metal–organic frameworks and their membranes, J Mater Chem A. 2018;6:5485-5506.
[35] Ataei F, Dorranian D, Motakef-Kazemi N. Bismuth-based metal–organic framework prepared by pulsed laser ablation method in liquid, JTAP. 2020;14:1-8.
[36] Ataei F, Dorranian D, Motakef-Kazemi N. Synthesis of MOF-5 nanostructures by laser ablation method in liquid and evaluation of its properties, J Mater Sci Mater Electron. 2021;32:3819-3833.

[37] Carné A, Carbonell C, Imaz I, Maspoch D. Nanoscale metal-organic materials, Chem Soc Rev. 2011;40(1):291-305.
[38] Berchel M, Le Gall T, Denis C, Le Hir S, Quentel F, Elléouet C, Montier T, Rueff JM, Salaün JY, Haelters JP, Hix GB. A silver-based metal-organic framework material as a 'reservoir' of bactericidal metal ions, NJC. 2011;35(5):1000-1003.
[39] Restrepo J, Serroukh Z, Santiago-Morales J, Aguado S, Gómez-Sal P, Mosquera ME, Rosal R. An antibacterial Zn-MOF with hydrazinebenzoate linkers, Eur J Inorg Chem. 2017;2017(3):574-580.
[40] Maji TK, Kitagawa S. Chemistry of porous coordination polymers, Pure Appl Chem. 2007;79(12):2155-2177.
[41] Venu Gopal VR, Kamila S. Effect of temperature on the morphology of ZnO nanoparticles: a comparative study, Appl Nanosci. 2017;7(3-4):75–82.
[42] Hajiashrafi S, Motakef-Kazemi N. Green synthesis of zinc oxide nanoparticles using parsley extract, Nanomed Res J. 2018;3(1):44–50.
[43] Sirelkhatim A, Mahmud S, Seeni A, Kaus NHM, Ann LC, Bakhori SKM, Hasan H, Mohamad D. Review on zinc oxide nanoparticles: antibacterial activity and toxicity mechanism, Nano-Micro Lett. 2015;7(3):219–242.